The Cerberus/Dan-family protein Charon is a negative regulator of Nodal signaling during left-right patterning in zebrafish

Hisashi Hashimoto[1,†], Michael Rebagliati[2], Nadira Ahmad[2], Osamu Muraoka[3], Tadahide Kurokawa[1], Masahiko Hibi[3]* and Tohru Suzuki[1]*

[1]National Research Institute of Aquaculture, Nansei, Mie 516-0193, Japan
[2]Department of Anatomy and Cell Biology, Roy J. and Lucille A. Carver College of Medicine, University of Iowa, Iowa City, Iowa 52242, USA
[3]Laboratory for Vertebrate Axis Formation, Center for Developmental Biology, RIKEN, Kobe 650-0047, Japan
*Authors for correspondence (e-mail: hibi@cdb.riken.jp and suzukitr@fra.affrc.go.jp)
†Present address: Bioscience and Biotechnology Center, Nagoya University, Nagoya 464-8601, Japan

Summary

We have isolated a novel gene, *charon*, that encodes a member of the Cerberus/Dan family of secreted factors. In zebrafish, *Fugu* and flounder, *charon* is expressed in regions embracing Kupffer's vesicle, which is considered to be the teleost fish equivalent to the region of the mouse definitive node that is required for left-right (L/R) patterning. Misexpression of Charon elicited phenotypes similar to those of mutant embryos defective in Nodal signaling or embryos overexpressing Antivin(Atv)/Lefty1, an inhibitor for Nodal and Activin. Charon also suppressed the dorsalizing activity of all three of the known zebrafish Nodal-related proteins (Cyclops, Squint and Southpaw), indicating that Charon can antagonize Nodal signaling. Because Southpaw functions in the L/R patterning of lateral plate mesoderm and the diencephalon, we asked whether Charon is involved in regulating L/R asymmetry. Inhibition of Charon's function by antisense morpholino oligonucleotides (MOs) led to a loss of L/R polarity, as evidenced by bilateral expression of the left side-specific genes in the lateral plate mesoderm (*southpaw*, *cyclops*, *atv/lefty1*, *lefty2* and *pitx2*) and diencephalon (*cyclops*, *atv/lefty1* and *pitx2*), and defects in early (heart jogging) and late (heart looping) asymmetric heart development, but did not disturb the notochord development or the *atv/lefty1*-mediated midline barrier function. MO-mediated inhibition of both Charon and Southpaw led to a reduction in or loss of the expression of the left side-specific genes, suggesting that Southpaw is epistatic to Charon in left-side formation. These data indicate that antagonistic interactions between Charon and Nodal (Southpaw), which take place in regions adjacent to Kupffer's vesicle, play an important role in L/R patterning in zebrafish.

Key words: Left/right asymmetry, Nodal, Cerberus/Dan family, Nodal flow, Zebrafish

Introduction

Establishment of left-right (L/R) patterning is one of the central processes of vertebrate embryogenesis. Studies in model animals show that some aspects of the mechanisms for L/R patterning are conserved among vertebrates (reviewed by Burdine and Schier, 2000; Hamada et al., 2001; Long et al., 2002; Wright, 2001; Wright and Halpern, 2002; Yost, 1998). It is believed that the breaking of L/R symmetry, which takes place near organizer derivatives, such as the definitive node in mouse and Hensen's node in the chicken, contributes to the L/R patterning, although there are several reports showing that L/R asymmetry is initiated at the beginning of development (Kramer et al., 2002; Levin and Mercola, 1999; Levin et al., 2002). In the mouse, cells on the ventral side of the definitive node have a monocilium that rotates in a counter-clockwise direction and generates a leftward flow of the extra-embryonic fluid (nodal flow) (Nonaka et al., 1998). Accumulated evidence from mouse studies suggest that the nodal flow plays a pivotal role in the L/R patterning (reviewed by Hamada et al., 2002; Tabin and Vogan, 2003). For example, inactivation of mouse

left-right dynein (*lrd*), which is expressed in the node cells, abolishes nodal flow and randomizes L/R asymmetry (McGrath et al., 2003; Okada et al., 1999; Supp et al., 1997). In zebrafish, an *lrd* homologue (left-right dynein-related; *lrdr*) appears at the late gastrula stage in dorsal forerunner cells that migrate ahead of the dorsal organizer region (Essner et al., 2002). The dorsal forerunner cells give rise to Kupffer's vesicle during the early segmentation stages (Cooper and D'Amico, 1996). Cells within Kupffer's vesicle have a cilium (Essner et al., 2002), suggesting a role for cilia in Kupffer's vesicle for L/R patterning.

The L/R-biased signals are thought to be transferred from the node to the lateral plate mesoderm (LPM), leading to the left side-asymmetric expression of *nodal*, *lefty* and the homeobox gene *pitx2* in the LPM. Nodal is a member of the transforming growth factor-β (TGF-β) family of cytokines and regulates the expression of *pitx2* and *lefty*, which encodes a feedback regulator for Nodal signaling in the left LPM (Essner et al., 2000; Liang et al., 2000; Shiratori et al., 2001; Yan et al., 1999; Yoshioka et al., 1998). Nodal also activates *nodal*

expression through an auto-regulation mechanism that involves the transcription factor FoxHl (Long et al., 2003; Norris et al., 2002; Osada et al., 2000; Saijoh et al., 2000). In zebrafish, Nodal signaling is also involved in the L/R patterning of the diencephalon (Concha et al., 2000; Gamse et al., 2003; Liang et al., 2000; Long et al., 2003). For the initiation of L/R patterning in the mouse, Nodal is required not only in the LPM, but also near the node (Brennan et al., 2002; Saijoh et al., 2003).

L/R asymmetry is maintained by midline barriers, which block the transfer of the left-side determinants. These midline barriers function either within the organizer itself or within differentiated derivatives of the midline organizer, such as the notochord and floor plate (Bisgrove et al., 2000; Lohr et al., 1997; Schlange et al., 2001). In zebrafish mutants *no tail*, *floating head* and *bozozok* (also known as *momo*) that perturb midline development, there is an increase in the incidence of the bilateral expression of left side-specific genes in the LPM (Bisgrove et al., 2000; Danos and Yost, 1996). Loss of Lefty1, which is expressed in the left floor plate, in mouse is reported to cause left isomerism (Meno et al., 1998).

In zebrafish, there are three known *nodal-related* genes, *cyclops* (*cyc*), *squint* (*sqt*) and *southpaw* (*spaw*). *cyc* and *spaw* are expressed in the left LPM (Long et al., 2003; Rebagliati et al., 1998a; Sampath et al., 1998). *cyc* is also expressed in the left diencephalon, in a region that corresponds to the prospective parapineal and pineal bodies (Liang et al., 2000; Rebagliati et al., 1998a; Sampath et al., 1998). *spaw* is also expressed near Kupffer's vesicle in a similar way to *nodal* expression near the node in mouse (Long et al., 2003). Mutations in the *cyc* gene have a minimal effect on visceral organ asymmetry (Bisgrove et al., 2000; Chen et al., 1997; Chin et al., 2000). However, several independent lines of evidence implicate Nodal signaling in the establishment of L/R asymmetry within the zebrafish. Loss of the late zygotic function of One-eyed pinhead (Oep), an EGF-CFC-family protein required for Nodal signaling, leads to defects in left-side gene expression and in visceral organ and diencephalic laterality (Gamse et al., 2003; Liang et al., 2000; Yan et al., 1999). Mutations in *schmalspur* (*sur*), which encodes FoxH1 and mediates Nodal signaling, also lead to defects in L/R patterning (Bisgrove et al., 2000; Chen et al., 1997; Pogoda et al., 2000; Sirotkin et al., 2000). Finally, antisense morpholino (MO)-mediated inhibition of Spaw disrupts the left-side expression of *cyc*, *pitx2*, *lefty1* and *lefty2* and leads to defects in L/R patterning in visceral organs and in the diencephalon (Long et al., 2003). *sqt* is not expressed asymmetrically, but in the absence of *sqt*, asymmetric expression of *spaw* is disrupted (Long et al., 2003). In sum, all of these data strongly implicate Nodal signaling in L/R patterning in the zebrafish, with *spaw* having a major role within the LPM and in at least the initial steps of diencephalic asymmetry.

Members of the Cerberus/Dan family have been implicated in L/R patterning by virtue of the asymmetric expression patterns of some of these proteins. In chick, for instance, *caronte* exhibits left-side expression within the paraxial mesoderm and LPM (Rodriguez Esteban et al., 1999; Yokouchi et al., 1999). Thus, Caronte has been postulated to transmit a signal from the node to the left LPM. Caronte can function as an inhibitor of BMP signaling (Rodriguez Esteban et al., 1999; Yokouchi et al., 1999). However, it was reported that BMP signaling positively regulates *nodal* expression in the left LPM by inducing an EGF-CFC protein that is required for the LPM's

competence to respond to Nodal ligands (Fujiwara et al., 2002; Piedra and Ros, 2002; Schlange et al., 2002; Schlange et al., 2001), raising the possibility that Caronte has functions other than inhibiting BMP signaling. Another member of the Cerberus/Dan family, Dante, is expressed around the node in mouse (Pearce et al., 1999). A role of Dante in L/R patterning has not yet been established.

Here we report the isolation of a novel gene, named *charon*, that encodes a Cerberus/Dan family secreted protein. *charon* is expressed from the early segmentation stages in the region embracing Kupffer's vesicle, adjacent and medial to the bilateral ('perinodal') *spaw*-expression domains. We found that Charon inhibits the activities of the Nodal-related proteins and identified Southpaw as a physiological target. Specifically, our data indicate that the antagonistic interaction between Charon and Nodal (Southpaw) plays an important role in L/R patterning in zebrafish.

Materials and methods

Fish embryos

Wild-type zebrafish (*Danio rerio*) embryos were obtained from natural crosses of fish from a pet shop and fish with the AB/India genetic background. *bozozok* (*boz*), *no tail* (*ntl*), *sqt*, *cyc* and *oep* were obtained after crossing fish heterozygous for the boz^{m168}, ntl^{b195}, sqt^{cz35}, cyc^{m294} or oep^{tz57} mutations. The *Fugu* and flounder embryos were prepared as described (Hashimoto et al., 2002; Suzuki et al., 2002).

Database searching and molecular cloning

Four distinct *Fugu* and zebrafish genes homologous to chick *caronte* were found in the NCBI database and in the *Fugu* (*Fugu rubripes*) genome database of the Doe Joint Genome Institute (http://fugu.jgi-psf.org) by a BLAST search. Three of these genes encoded proteins with strong homology to Cerberus/Caronte, PRDC and Gremlin. The other was distantly related to any of the known Cerberus/Dan family proteins. Here, we describe the isolation of *Fugu*, zebrafish and flounder cDNAs of the gene *charon*, whose protein displayed the strongest homology to Cerberus/Caronte. The *Fugu charon* cDNA containing the whole open reading frame (ORF) was amplified by PCR with the following primer set: sense, 5′-CGGGATCCCA-GACGACAATTTTCCTGTTG-3′, and antisense, 5′-CCATCGATG-CAGGCGTCCCGAAGCTGCGT-3′. The resulting fragment was cloned into pBluescript II (pBS-fugu-charon). The cDNA fragment of zebrafish *charon* was isolated from a segmentation stage (15 hours post-fertilization, 15 hpf) cDNA library, which was constructed using a Marathon cDNA library synthesis kit (Clontech), with 5′ and 3′ RACE using the primers 5′-GGTTTCACACTTGCACTCCTC-AACG-3′ and 5′-GCACTCCTCAACGATCAGTACGCACC-3′ for 5′ RACE, and 5′-CAGCGCATAACGGAGGAGGGCTGTG-3′ and 5′-GGAGGGCTGTGAGACGGTGACCGTT-3′ for 3′ RACE. The resulting fragment was subcloned into pDrive (Qiagen) (pDrive-zcharon for the 5′ RACE clone). After determining the 5′- and 3′ ends of the full-length charon cDNA, the zebrafish *charon* ORF was amplified by PCR with the following primers: sense, 5′-CGGGAT-CCCGAAACCTTGAACCGCAAGATT-3′, and antisense, 5′-CCAT-CGATGTAAATTAAACATATCTGTGTT-3′. The resulting fragment was cloned into pCS2MT or pCS2 (pCS2MT-zcharon or pCS2-zcharon). A part of the flounder *charon* cDNA was obtained by PCR with primers that corresponded to the conserved amino acids RVTAAGC and ETGREEK: sense, 5′-AGCGTGTGACGGCGGCG-GGATG-3′, and antisense, 5′-CCTTTTCCTCGCGGCCTGTTTC-3′. The obtained fragment was verified by sequencing. Using this fragment as a probe, a putative full-length clone of flounder *charon* was isolated from a lambda ZipLox cDNA library of 20-somite flounder embryos,

and the lambda phage clone was converted to the plasmid (pZL-fl-charon). The nucleotide sequences of zebrafish *charon*, *Fugu charon* and flounder *charon* were deposited in the DDBJ databank under accession numbers AB110416, AB110417 and AB1100418, respectively. Zebrafish PRDC and gremlin will be published elsewhere.

Constructs, RNA synthesis and transcript detection

pcDNA3.1-Charon-Myc was constructed by insertion of the Charon-Myc fragment (a Myc tag in the carboxy terminal) from pCS2MT-zcharon into the *Bam*HI and *Eco*RI sites of pcDNA3.1. pcDNA3.1-PRDC-Myc was constructed in a similar manner to that for pcDNA3.1-Charon-Myc. pcDNA3.1-HA-Spaw was constructed by insertion of the *Eco*RI-*Not*I fragment from pCS2+ActHASpaw (Long et al., 2003) into pcDNA3.1. pBS-fugu-charon was used for in situ hybridization of the *Fugu* embryo. A DIG-labeled riboprobe was made with T3 RNA polymerase (Promega) after *Not*I digestion. pZL-fl-charon was used for the flounder embryo. A DIG-labeled riboprobe was made with SP6 RNA polymerase (Promega) after *Sal*I digestion. The zebrafish riboprobe was made with *Bam*HI-digested pDrive-zcharon using SP6 RNA polymerase (Promega). Synthetic zebrafish *charon* RNA was produced with pCS2MT-zcharon or pCS2-zcharon. After *Not*I digestion, the RNA for Myc-tagged Charon or untagged Charon was transcribed in a solution containing an RNA cap structure analog (New England BioLabs) and SP6 RNA polymerase (Promega). Synthesis of RNAs for *cyc, sqt* and *spaw* was performed as described previously (Long et al., 2003; Rebagliati et al., 1998a; Rebagliati et al., 1998b). The method for detecting *spaw*, *cyc*, *ntl*, *goosecoid*, *six3.2*, *pax2.1*, *nkx2.5* and *cardiac myosin light chain* (*cmlc2*) expression was also previously published (Chen and Fishman, 1996; Hashimoto et al., 2000; Long et al., 2003; Yelon et al., 1999). Whole-mount in situ hybridization and two-color staining were performed as described (Hashimoto et al., 2000; Long et al., 2003; Long and Rebagliati, 2002).

Interaction assay

COS7 cells in a 10 cm-diameter dish (approximately 10^6 cells) were transfected with 10 µg of pcDNA3.1-Charon-Myc, pcDNA3.1-PRDC-Myc or pcDNA3.1-HA-Spaw by a standard calcium phosphate precipitation method. After 20 hours, the medium was changed from 10% fetal calf serum-contained DMEM to serum-free Opti-MEM1 (Invitrogen). After 48 hours, the supernatants were harvested. The supernatants containing Charon-Myc (25 µl), PRDC-Myc (25 µl) or HA-Spaw (250 µl) were mixed in a combination described in Fig. 5 and incubated with anti-Myc (9E10, Invitrogen) or anti-HA (3F10, Roche) antibodies, and protein G sepharose, at 4°C for 15 hours. The precipitates were washed five times with washing buffer: 20 mM Tris-HCl, pH 7.5, 150 mM NaCl, 0.1% Triton X-100, proteinase inhibitor Complete Mini EDTA-free (Roche), eluted with Laemmli's sodium dodecyl sulfate (SDS) loading buffer, and separated on an SDS-4 to 20% gradient polyacrylamide gel. The immune complexes were visualized by a chemiluminescence system (Western Lightning; PerkinElmer Life Sciences).

Morpholino oligonucleotides

The antisense MOs were generated by Gene Tools (LLC, Corvallis, OR, USA). For the *charon*-MOs, the sequences were: *charon*-MO, 5′-CAAAAAAGCCGACCTGAAAAGTCAT-3′, and 4mis-MO, 5′-CAtAAAtGCCGACCTGAtAAGaCAT-3′ (lower case letters indicate mis-paired bases). The *spaw*-MO was previously published (*spaw*-MO1) (Long et al., 2003). The MOs were dissolved in and diluted with 1× Danieau's buffer (Nasevicius and Ekker, 2000).

Results

Isolation of a novel teleost gene for a Cerberus/Caronte/Dan family protein

We are interested in elucidating how the node/organizer initiates L/R asymmetry within the LPM in the teleost embryo. To this end, we attempted to isolate fish homologues of chick *caronte*, which is reported to mediate a signal for left-side formation that is sent by the node to the left LPM (Rodriguez Esteban et al., 1999; Yokouchi et al., 1999). We searched a *Fugu* (*Fugu rubripes*) genome database and found one transcription unit deduced from the genome sequence that displayed a relatively strong homology to chick *caronte*. We named the gene *charon* and isolated the full-length *charon* cDNA by PCR. We found a partial coding fragment of zebrafish *charon* in the NCBI database (Z35724-a1466a08.p1c), and isolated the full-length cDNA of zebrafish *charon* by 5′ and 3′ RACE using the sequence information. We also isolated a flounder *charon* cDNA by combining degenerate PCR and a hybridization screen. The ORFs of the *charon* cDNAs consisted of 729 bp (zebrafish), 765 bp (*Fugu*) and 786 bp (flounder); they encoded 243, 255 and 262 amino acid residues, respectively. The zebrafish Charon protein exhibited a 42% amino acid identity to both the *Fugu* and flounder Charon proteins (Fig. 1A). In addition to the sequence similarities, the expression profiles of the *Fugu*, zebrafish and flounder *charon* genes were relatively similar to each other (Fig. 2), suggesting that they are orthologues.

The nine cysteine residues in the cysteine knot domain that are conserved among the Cerberus/Dan family were also conserved in Charon, indicating that Charon is a member of the Cerberus/Dan family. Within the cysteine knot domain, the zebrafish Charon protein had stronger similarities to *Xenopus* Cerberus (18%), chick Caronte (25%) and human Cerberus-related (20%) than to Dante or the other members of the Cerberus/Dan family (Fig. 1B). Outside of the cysteine knot domain, Charon did not have an apparent similarity to other Cerberus/Dan family proteins.

charon expression

charon transcripts were first detected at the beginning of somitogenesis (2-3 somite stages) in the hypoblast of the tailbud region in zebrafish (Fig. 2A,B). At the 10-somite stage (14 hpf), the expression domain was observed as a horseshoe-shaped zone (with the anterior side open) in the tail region (Fig. 2C,D). Sagittal sectioning revealed that the *charon*-expressing cells were either within the epithelial lining of Kupffer's vesicle or very closely apposed to Kupffer's vesicle (Fig. 5M). The expression was strongest at the 10-somite through to the 14-somite stage (16 hpf) (Fig. 2G,H), then gradually disappeared, and it was not detected at 24 hpf. *charon* was not detected anywhere besides the region adjacent to Kupffer's vesicle at any developmental stage. *charon* was expressed in the region adjacent to Kupffer's vesicle in *Fugu* and flounder embryos, as in zebrafish (Fig. 2I-L).

We next examined the regulation of *charon* expression using the zebrafish mutants *boz*, *ntl*, *cyc*, *sqt* and *oep*. *boz* mutant embryos display variable defects in dorso-axial structures including the dorsal forerunner cells, which give rise to Kupffer's vesicle (Fekany et al., 1999). In *boz* mutant embryos, *charon* expression was reduced or not detectable, with a variable penetrance (Fig. 3B,C). The *charon* expression was not detected in the *ntl* mutant embryos (Fig. 3D), which display defective development of the dorsal forerunner cells, notochord and tail (Melby et al., 1996). The *charon* expression was not affected in the *cyc* mutant embryos (Fig. 3G), but it was
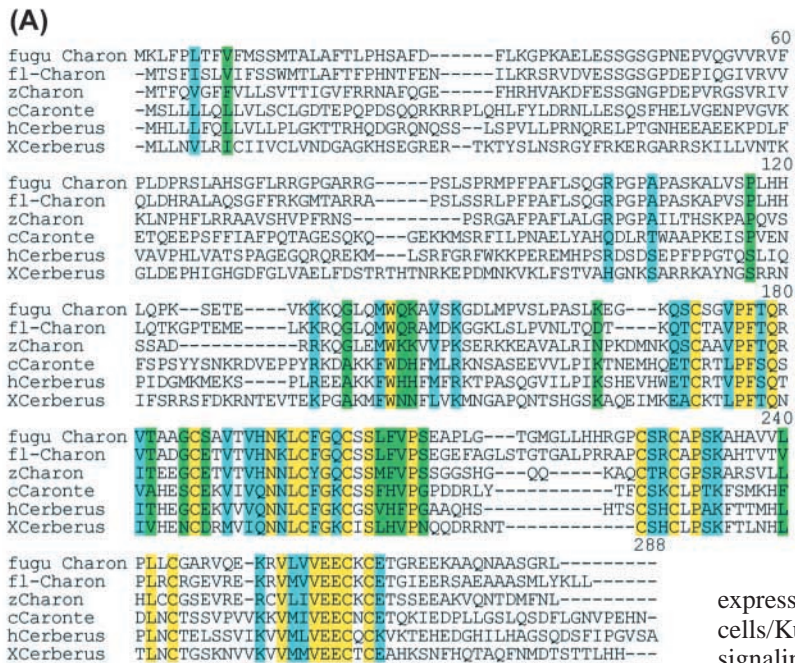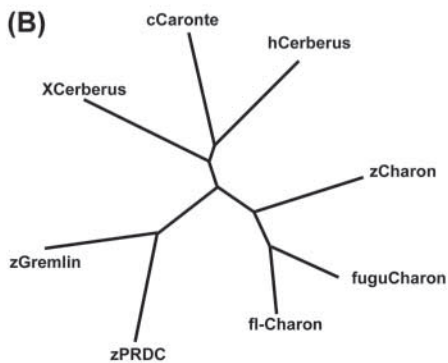
(A)

```
                          60
fugu Charon  MKLFPLTFVFMSSMTALAFTLPHSAFD------FLKGPKAELESSGSGPNEPVQGVVRVF
fl-Charon    -MTSFISLVIFSSWMTLAFTFPHNTFEN-----ILKRSRVDVESSGSGPDEPIQGIVRVV
zCharon      -MTFQVGFFVLLSVTTIGVFRRNAFQGE-----FHRHVAKDFESSGNGPDEPVRGSVRIV
cCaronte     -MSLLLLQLLVLSCLGDTEPQPDSQQRKRRPLQHLFYLDRNLLESQSFHELVGENPVGVK
hCerberus    -MHLLLFQLLVLLPLGKTTRHQDGRQNQSS--LSPVLLPRNQRELPTGNHEEAEEKPDLF
XCerberus    -MLLNVLRICIIVCLVNDGAGKHSEGRER--TKTYSLNSRGYFRKERGARRSKILLVNTK
                                                                 120
fugu Charon  PLDPRSLAHSGFLRRGPGARRG-----PSLSPRMPFAFLSQGRPGPAPASKALVSPLHH
fl-Charon    QLDHRALAQSGFFRKGMTARRA-----PSLSSRLPFPAFLSQGRPGPAPASKAPVSPLHH
zCharon      KLNPHFLRRAAVSHVPFRNS----------PSRGAFPAFLALGRPGPAILTHSKPAPQVS
cCaronte     ETQEEPSFFIAFPQTAGESQKQ---GEKKMSRFILPNAELYAHQDLRTWAAPKEISPVEN
hCerberus    VAVPHLVATSPAGEGQRQREKM---LSRFGRFWKKPEREMHPSRDSDSEPFPPGTQSLIQ
XCerberus    GLDEPHIGHGDFGLVAELFDSTRTHTNRKEPDMNKVKLFSTVAHGNKSARRKAYNGSRRN
                                                              180
fugu Charon  LQPK--SETE-----VKKKQGLQMWQKAVSKGDLMPVSLPASLKEG---KQSCSGVPFTQR
fl-Charon    LQTKGPTEME----LKKRQGLQMWQRAMDKGGKLSLPVNLTQDT----KQTCTAVPFTQR
zCharon      SSAD-----------RRKQGLEMWKKVVPSERKKEAVALRINPKDMNKQSCAAVPFTQR
cCaronte     FSPSYYSNKRDVEPPYRKDAKKFWDHFMLRKNSASEEVVLPIKTNEMHQETCRTLPFSQS
hCerberus    PIDGMKMEKS----PLREEAKKFWHHFMFRKTPASQGVILPIKSHEVHWETCRTVPFSQT
XCerberus    IFSRRSFDKRNTEVTEKPGKAMFWNNFLVKMNGAPQNTSHGSKAQEIMKEACKTLPFTQN
                                                            240
fugu Charon  VTAAGCSAVTVHNKLCFGQCSSLFVPSEAPLG---TGMGLLHHRGPCSRCAPSKAHAVVL
fl-Charon    VTADGCETVTVHNKLCFGQCSSLFVPSEGEFAGLSTGTGALPRRAPCSRCAPSKAHTVTV
zCharon      ITEEGCETVTVHNNLCYGQCSSMFVPSSGGSHG---QQ-----KAQCTRCGPSRARSVLL
cCaronte     VAHESCEKVIVQNNLCFGKCSSFHVPGPDDRLY----------TFCSKCLPTKFSMKHF
hCerberus    ITHEGCEKVVVQNNLCFGKCSSFHVPGAAQHS----------HTSCSKCLPAKFTTMHL
XCerberus    IVHENCDRMVIQNNLCFGKCISLHVPNQQDRRNT----------CSHCLPSKFTLNHL
                                              288
fugu Charon  PLLCGARVQE-KRVLVVEECKCETGREEKAAQNAASGRL---------
fl-Charon    PLRCRGEVRE-KRVMVVEECKCETGIEERSAEAAASMLYKLL------
zCharon      HLCCGSEVRE-RCVLIVEECKCETSSEEAKVQNTDMFNL---------
cCaronte     DLNCTSSVPVVKKVMIVEECNCETQKIEDPLLGSLQSDFLGNVPEHN-
hCerberus    PLNCTELSSVIKVVMLVEECQCKVKTEHEDGHILHAGSQDSFIPGVSA
XCerberus    TLNCTGSKNVVKVVMMVEECTCEAHKSNFHQTAQFNMDTSTTLHH---
```

(B)

Fig. 1. Comparison of the amino acid sequence of fish Charon with the sequences of other Cerberus/Dan family members. (A) Alignment was done with the ClustalW program. Identities in the amino acid sequence of zebrafish (z) Charon to the sequences *Fugu* Charon, flounder (fl) Charon, *Xenopus* (X) Cerberus, chick (c) Caronte, and human Cerberus-related (hCerberus) are 41%, 41%, 18%, 25%, 20%, respectively. *Fugu* Charon and flounder Charon are the most similar to each other (63%). (B) A radial phylogenic tree of the Cerberus/Dan family proteins. The tree was calculated according to the Expansion of the ClustalW program by DDBJ (DDBJ; http://www.ddbj.nig.ac.jp) using the amino acid sequences of the cysteine-knot domain of the proteins. Zebrafish PRDC and zebrafish Gremlin are less similar (16% and 18%, respectively) to chick Caronte than to zebrafish Charon. c, chick; X, *Xenopus*; z, zebrafish.

expression depends on the formation of the dorsal forerunner cells/Kupffer's vesicle, which is dependent on the Nodal signaling.

Charon functions as an inhibitor of Nodal signaling

Cerberus/Dan-family proteins are inhibitors for TGF-β family proteins such as BMPs and a Nodal, and for Wnt proteins (Bell et al., 2003; Pearce et al., 1999; Piccolo et al., 1999; Rodriguez Esteban et al., 1999; Yokouchi et al., 1999). To investigate the function of Charon, we misexpressed *charon* RNA in zebrafish embryos. The RNA injection led to variable levels of defects in the formation of mesendoderm. The phenotypes were classified into three categories (Class I-III) with increasing severity (Fig. 4, Table 1). Class I embryos displayed a slightly shortened axial structure at 10 hpf (the time of yolk plug closure, YPC) (Fig. 4E), lacked the prechordal plate, had fused eyes and reduced notochord structure at the pharyngula stage (24 hpf, Fig. 4F-I). The phenotypes were similar to those observed in mutants with mildly affected Nodal signaling, such as zygotic *oep* and maternal-zygotic (MZ) *sur* (lacking maternal and zygotic Sur protein) (Pogoda et al., 2000; Sirotkin et al., 2000; Solnica-Krezel et al., 1996), or in embryos injected with a small amount of *atv/lefty1* RNA. Class II embryos exhibited a severe defect in dorsal axis extension at YPC (Fig. 4J), and displayed a cyclopic eye, reduced trunk somites and loss of the notochord at the pharyngula stage (Fig. 4K-M). Class III embryos displayed a lack of dorsal axis extension and had a dorsal vegetal mass at YPC (Fig. 4N). They had a cyclopic eye, but lacked most mesoderm and endoderm at the

reduced or absent in the *sqt* mutant embryos, which exhibit defective development of Kupffer's vesicle (Dougan et al., 2003) (Fig. 3E,F). In the *oep* mutant embryos, the *charon* expression was comparable to that in the wild-type embryos, but the expression domain was smaller than that in the wild-type embryos, in proportion to the size of Kupffer's vesicle (Fig. 3H). The *charon* expression was not detected in embryos injected with a large amount of RNA for the Nodal/Activin inhibitor Atv/Lefty1 (Thisse and Thisse, 1999) (Fig. 3I). The *atv/lefty1* RNA-injected embryos did not have Kupffer's vesicle (data not shown). The data suggest that *charon*

Table 1. Effects of misexpression of *charon*

	RNA	Morpholino	Dose	n	Normal	(%)		
						Class I	Class II	Class III
Experiment 1	*charon*		25 pg	86	0	5	72	23
	charon		100 pg	106	0	1	18	81
Experiment 2	*charon*		25 pg	29	0	3	55	41
	charon	*charon*-MO	25 pg+0.8 ng	51	90	10	0	0

charon RNA, or *charon* RNA and *charon*-MO were injected into one- to two-cell stage embryos and the embryos were classified into three categories (Class I-III) by morphological inspection (Fig. 4) at 10 hpf (yolk plug closure) and 24 hpf.
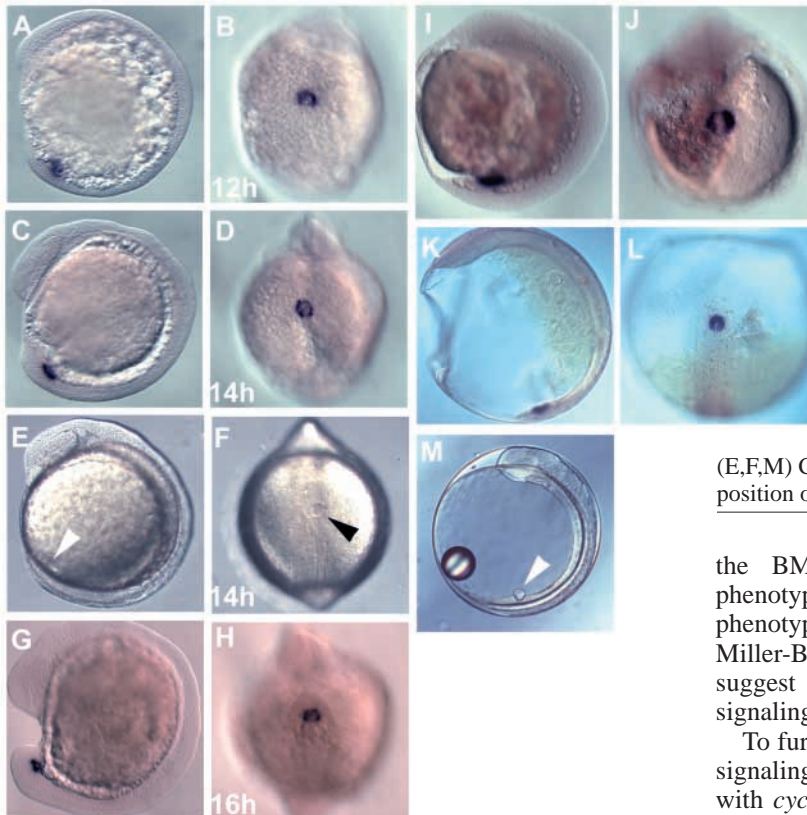
Fig. 2. *charon* expression in zebrafish. In situ hybridization analysis revealed that *charon* expression was initiated around 12 hpf at the 6-somite stage in the tailbud (A,B). *charon* expression became more obvious at 14 hpf (10-somite stage) (C,D). The *charon* transcripts were observed in the posterior half of the flanking domain of Kupffer's vesicle in a horseshoe shape (D, refer to E,F). The expression continued through 15 hpf to 18 hpf in the same tissue (16 hpf, 14-somite stage, G,H). The expression pattern of *charon* mRNA in *Fugu* (I,J) and flounder (K,L, refer to M) was very similar to that in zebrafish. The *charon* transcripts were not detected in any other domain throughout embryogenesis. There was no obvious L/R bias in the strength of *charon* expression in the majority of embryos. (A,C,E,G,I,K,M) Lateral views. (B,D,F,H,J,L) Vegetal pole views of the tailbud region. (E,F,M) Control non-stained embryos. Arrowheads indicate the position of Kupffer's vesicle.

the BMP inhibitors Noggin1 and Chordin (dorsalized phenotypes), or the Wnt inhibitor Dkk1 (anteriorized phenotypes) (Furthauer et al., 1999; Hashimoto et al., 2000; Miller-Bertoglio et al., 1997; Shinya et al., 2000). These data suggest that Charon functions as an inhibitor for Nodal signaling.

To further confirm an antagonistic role for Charon in Nodal signaling, we expressed *charon* RNA alone, or *charon* RNA with *cyc*, *sqt* or *spaw* RNA, and examined the expression of various genetic markers (Figs 4, 5). Misexpression of *charon* abolished *goosecoid* (*gsc*) and *ntl* expression in the dorsal axial mesendoderm as well as a posterior expansion of the forebrain marker *six3.2* (Fig. 4S,U,W,Y). All of these expression profiles are similar to those observed in MZ*oep* and *cyc;sqt* mutant embryos and in *atv/lefty1* RNA-injected embryos (Feldman et al., 1998; Gritsman et al., 1999; Meno et al., 1999; Thisse and Thisse, 1999). Injection of *cyc* (10 pg), *sqt* (10 pg) or *spaw* (100 pg) RNA led to dorsalization (data not shown), expansion and/or ectopic expression of *gsc* (Fig. 5A,C,E). Co-injection of 25 pg of *charon* RNA with these *nodal* RNAs suppressed the dorsalization, expansion and ectopic expression of *gsc* that were elicited by the *nodal* RNA injection (Fig. 5B,D,F). We also found that Charon but not PRDC (another member of the Cerberus/Dan family) interacted with Spaw (Fig. 5G). Taking these observations together with the phenotypes of the *charon*-
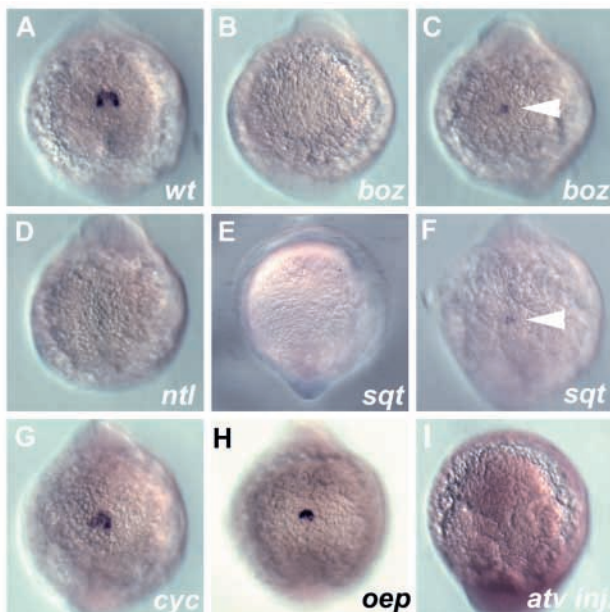
phayngula stage (Fig. 4O-Q), as observed in MZ*oep* embryos, *cyc;sqt* double mutant embryos, or embryos injected with a large amount of *atv/lefty1* RNA (Feldman et al., 1998; Gritsman et al., 1999; Meno et al., 1999; Pogoda et al., 2000; Sirotkin et al., 2000; Solnica-Krezel et al., 1996), which are more completely deficient in Nodal signaling. The effects of the *charon* RNA injection depended on the dose of the injected RNA (Table 1). The phenotypes of *charon*-misexpressing embryos were different from those of embryos misexpressing

Fig. 3. Regulation of *charon* expression. Expression of *charon* in the wild-type (A), mutant (B-H) and *antivin/lefty1* RNA-injected (*atv* inj.) embryos (I) at the 10-somite stage (13 hpf). Vegetal pole views of the tailbud region. In *bozozok* (*boz*) embryos, *charon* expression was reduced (C) or absent (B). In *no tail* (*ntl*) embryos, no *charon* expression was detected (D). In *squint* (*sqt*) embryos, *charon* expression was reduced (F) or absent (E). In *cyclops* (*cyc*) embryos, *charon* expression was not affected (G). In *one-eyed pinhead* (*oep*) embryos, the strength of *charon* expression was not affected, but the expression domain became smaller, in proportion to the size of Kupffer's vesicle (G). In embryos injected with 25 pg of *antivin/lefty1* RNA, which displayed phenotypes similar to *cyc:sqt* double mutant and maternal-zygotic *oep* mutant embryos at 24 hpf (data not shown), no *charon* expression was detected (I). Variability of *charon* expression in *boz* and *sqt* embryos was consistent with the variable expressivity of these *boz* and *sqt* alleles. Arrowheads indicate weak expression of *charon*.
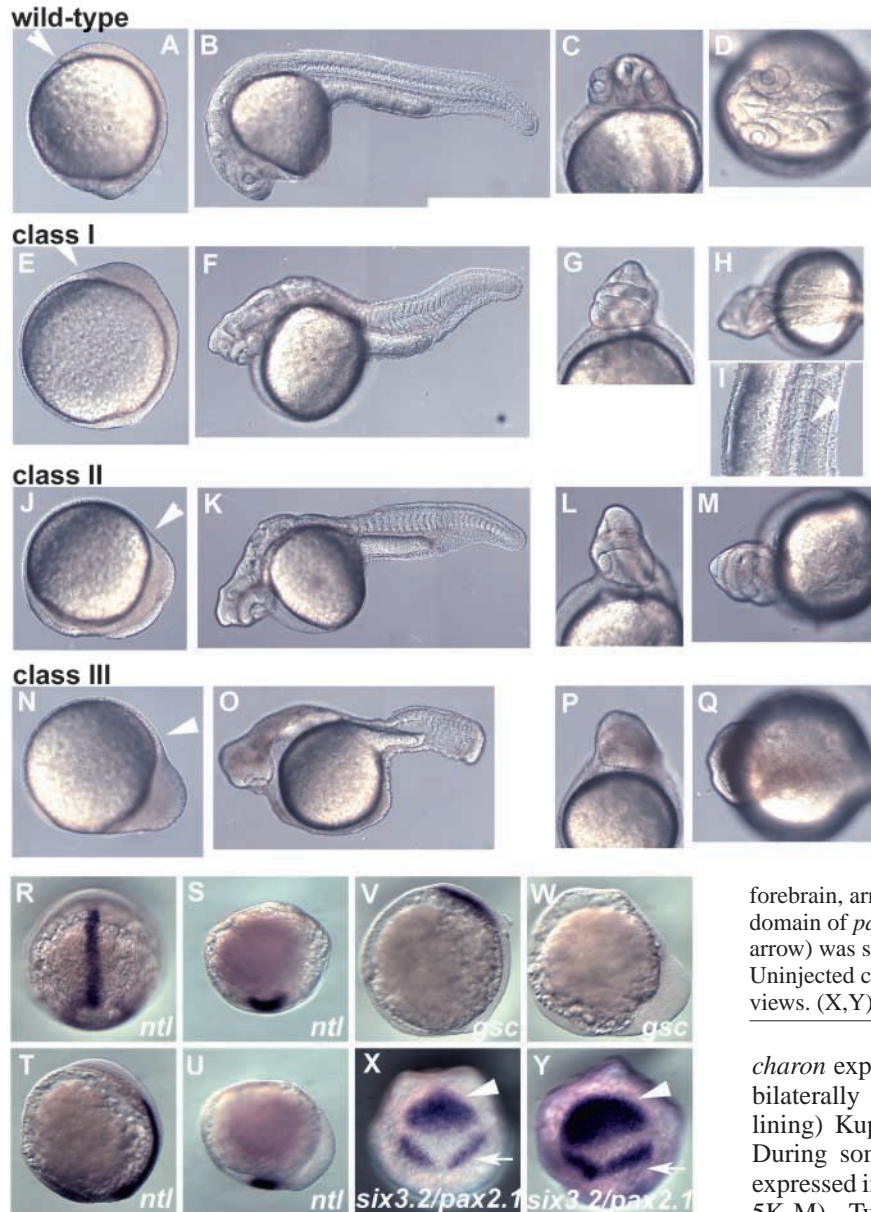
Fig. 4. Overexpression of zebrafish *charon* leads to a lack of mesendoderm. Zebrafish *charon* RNA (25 or 100 pg) was injected into one-to-four cell stage embryos. The RNA injection led to variable levels of defects in the formation of mesendoderm, which is observed in *one-eyed pinhead* (*oep*) mutant and *antivin/lefty1*-injected embryos. Non-injected control embryos at 10 hpf [at the time of yolk plug closure (YPC), which is equivalent to bud stage (A) and at the pharyngula stage (24 hpf, B,C,D)]. The phenotypes of the injected embryos were classified into three categories (Class I-III) with increasing severity. Class I embryos at YPC (E) and at the pharyngula stage (F-I). Class II embryos at YPC (J) and at the pharyngula stage (K,L,M). Class III embryos at YPC (N) and at the pharyngula stage (O,P,Q). (A,B,E,F,J,K,N,O) Lateral views. (C,G,L,P) Ventral views of the head. (D,H,M,Q) Dorsal views of the head. (I) Lateral view of the trunk. Arrowheads indicate the anterior border of the dorsal axial mesendoderm and notochord. The numbers of each class of the embryos are shown in Table 1. (R-Y) Misexpression of *charon* caused a defect in the axial mesendoderm formation. The embryos receiving 25 pg of *charon* RNA lacked *no tail* (*ntl*) expression in the dorsal midline and dorsal forerunner cells at YPC (S,U) and *goosecoid* (*gsc*) expression at the 90% epiboly stage (W). In the *charon* RNA-injected embryos, the expression of *six3.2* (a marker for forebrain, arrowhead) was slightly expanded and the expression domain of *pax2.1* (a marker for the mid-hindbrain boundary, arrow) was slightly shifted posteriorly at YPC (Y). (R,T,W,X) Uninjected control embryos. (R,S) Dorsal views. (T-W) Lateral views. (X,Y) Animal pole views, with ventral to the top.

misexpressing embryos, we conclude that Charon functions as an inhibitor for Nodal signaling.

charon and *spaw* are expressed in an adjacent region near Kupffer's vesicle

Charon inhibited all the Nodal-related proteins in zebrafish in the misexpression studies. To address which Nodal-related ligand(s) is the physiological target for Charon, we first compared the expression profiles of *charon* and the *nodal*-related genes. *sqt* expression did not overlap with *charon* expression at any developmental stage (data not shown). *cyc* is expressed in the tailbud region at the bud stage, but its expression disappears by the 2-3 somite stage (Rebagliati et al., 1998a; Sampath et al., 1998), indicating that the expression of *cyc* coincides with that of *charon* spatially but not temporally. *spaw* displays a similar expression to *charon* in the tailbud region (Long et al., 2003); *spaw* expression is first detectable at the 4-6-somite stage (14 hpf), slightly later than the initial

charon expression. The *spaw*-expressing cells were located bilaterally in two domains flanking (or possibly in cells lining) Kupffer's vesicle (Long et al., 2003) (Fig. 5H-J). During somitogenesis, *spaw* and *charon* continued to be expressed in adjacent regions close to Kupffer's vesicle (Fig. 5K-M). Two-color staining and examinations of cross-sectioned embryos revealed that the *spaw*-expressing cells were located dorsal and lateral to the *charon*-expressing cells (Fig. 5N-Q). The expression domains of *spaw* and *charon* did not overlap. However, both genes encoded secreted proteins, so their domains could overlap at the level of protein. The expression of both genes was maintained until the end of somitogenesis (data not shown). These data indicate that Spaw is the best candidate for a functional target for Charon.

Knockdown of Charon leads to a defect in heart positioning

We performed loss-of-function experiments by injecting antisense MOs against the translational initiation site of *charon* (*charon*-MO, Fig. 6). To examine the specificity of *charon*-MO, we co-injected *charon*-MO with *charon* RNA into embryos. The phenotypes caused by the misexpression of *charon* were suppressed by the co-injection of *charon*-MO (Fig. 6A,B, Table 1). Embryos injected with *charon*-MO alone (*charon* morphant embryos) did not show any gross
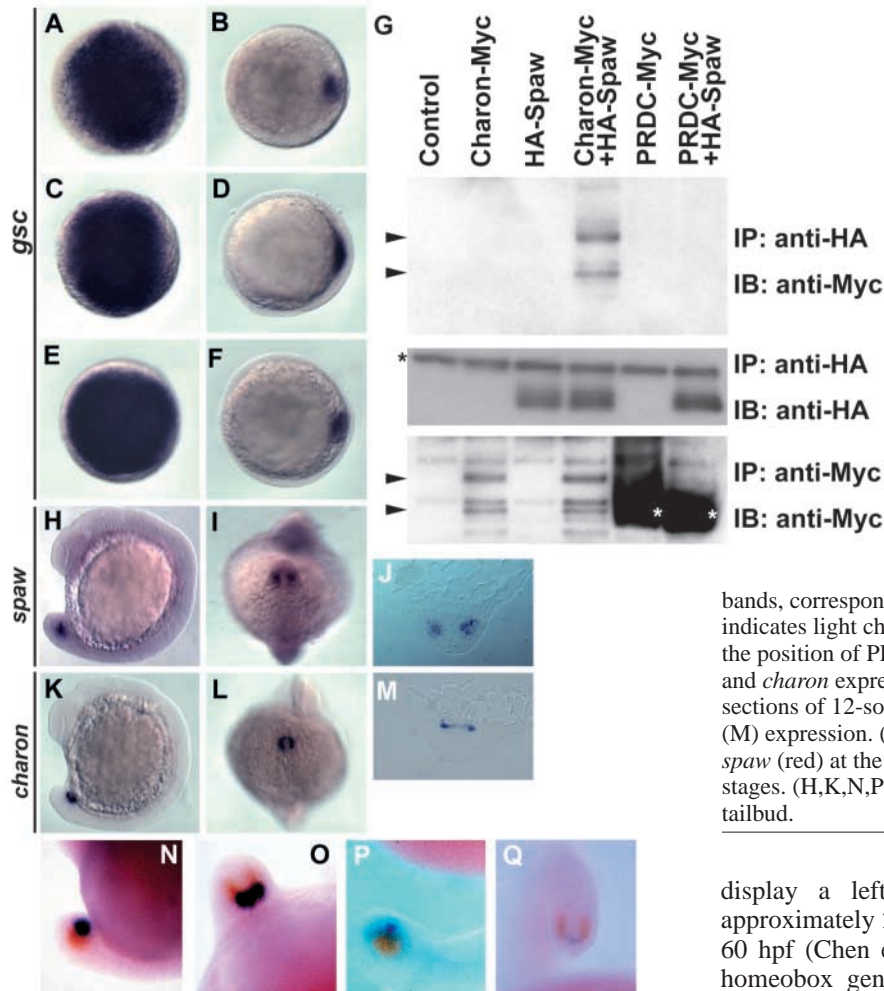
Fig. 5. Charon inhibits Nodal signaling. (A-F) Overexpression of Charon inhibited the effects of Nodal overexpression. The injection of 10 pg of *cyclops* (*cyc*) or *squint* (*sqt*) RNA, or 100 pg of *southpaw* (*spaw*) RNA elicited expansion and/or ectopic expression of *goosecoid* (*gsc*) at 6 hpf (A,C,E). Co-injection of 25 pg *charon* RNA inhibited the effects of *cyc, sqt* and *spaw* overexpression (B,D,F). (A-F) Animal pole views, with dorsal to the right. (G) Interaction between Charon and Southpaw. COS7 cells were transfected with expression vectors for Myc-tagged Charon (Charon-Myc), Myc-tagged PRDC (PRDC-Myc), or HA-tagged Spaw (HA-Spaw). The supernatants containing Charon-Myc, PRDC-Myc and HA-Spaw were mixed as indicated, and immunoprecipitated with anti HA- or anti-Myc epitope antibodies. The immunoprecipitates were immunoblotted with anti-HA or Myc antibodies. Arrowheads indicate the position of Charon-Myc (two bands, correspond to approximately 35 and 40 kD). A black asterisk indicates light chains of the antibodies, and white asterisks indicate the position of PRDC-Myc. (H-M) *southpaw* (*spaw*) expression (H,I) and *charon* expression (K,L) at the 12-somite stage (15 hpf). Cross-sections of 12-somite stage embryos showing *charon* (J) and *spaw* (M) expression. (N-Q) Two-color staining of *charon* (purplish) and *spaw* (red) at the 12 somite (N,O) and 18-somite (18 hpf; P,Q) stages. (H,K,N,P) Lateral views. (I,L,O,Q) Dorsal views of the tailbud.

morphological abnormalities during early development and survived for at least 1 week after hatching (Fig. 6L). However, we found that the *charon* morphant embryos displayed abnormal positioning of the heart (Fig. 6C-K, Table 2). The process of heart positioning can be divided into two steps, jogging and looping (Chen et al., 1997); jogging and looping are two aspects of heart L/R asymmetry. Wild-type embryos

display a leftward shift (jog) of the heart tube from approximately 26-30 hpf and rightward (D-) looping from 30-60 hpf (Chen et al., 1997) (Table 2). The expression of the homeobox gene *nkx2.5* and a cardiac-specific *myosin light chain* (*cmlc2*) gene can be used to visualize the jogging and looping of the heart (Chen and Fishman, 1996; Yelon et al., 1999). Using these markers, we found that the laterality of the heart jogging was severely perturbed in the *charon* morphant embryos, but not in the control morphant embryos (Fig. 6C-H, Table 2). Likewise, heart looping was disrupted in *charon* morphant embryos, as shown by significant increases in the fraction of embryos with reversed heart loops (L-loops) or unlooped hearts (Fig. 6I-K, Table 2). These data indicate that

Table 2. Charon is required for heart jogging and looping

| | Morpholino | Dose (ng) | Marker | Stage (hpf) | *n* | Jogging (%) | | |
						L-jog	No-jog	R-jog
Experiment 1	4-Mis	0.8	*cmlc2*	26	126	98	1	1
	charon-MO	0.8	*cmlc2*	26	122	61	13	26
Experiment 2	4-Mis	0.8	–	30	22	90	5	5
	charon-MO	0.8	–	30	80	53	26	21
						Looping (%)		
						D-loop	No-loop	L-loop
Experiment 3	None	0	*cmlc2*	52	9	100	0	0
	4-Mis	0.8	*cmlc2*	52	23	92	4	4
	charon-MO	0.8	*cmlc2*	52	42	66	17	17

charon-MO or control MO (4-Mis), which contains four mispaired nucleotide in the MO recognition sequence, was injected and the embryos were fixed at the indicated stages. Jogging and looping of the hearts were determined by observing the cardiac myosin light chain (*cmlc2*)-stained embryo (at 26 hpf and 52 hpf, Fig. 6) or the living embryos (30 hpf).

Charon is involved in L/R-biased heart positioning during heart formation.

Charon is required for early L/R patterning processes

To investigate how early the loss of Charon affects the L/R patterning, we analyzed the expression of the left side-specific genes, *atv/lefty1, lefty2, pitx2, cyc* and *spaw*. The *nodal-related* gene *spaw* is the earliest marker of embryonic L/R asymmetry in the zebrafish embryo and is required globally for correct L/R asymmetry (Long et al., 2003). Thus, changes in *spaw* expression provide an indicator of the general degree of disruption of overall L/R patterning. The *charon* morphant
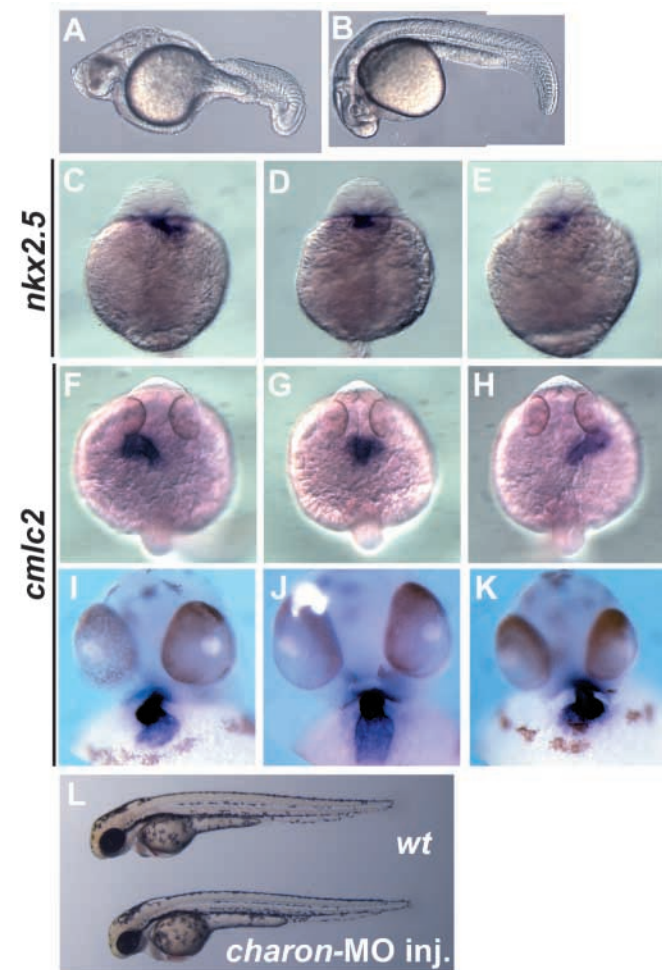
Fig. 6. Knockdown of Charon leads to a defect in heart laterality. (A) A pharyngula-stage (24 hpf) embryo that received 25 pg of *charon* RNA. (B) An embryo that received both *charon* RNA (25 pg) and *charon*-MO (0.8 ng). (C-K) The *charon* morphant embryos displayed variable defects in heart positioning. The numbers of embryos showing each phenotype are shown in Table 2. *nkx2.5* expression at 26 hpf (C-E), and *cardiac myosin light chain* (*cmlc2*) expression at 26 hpf (F-H) and 52 hpf (I-K). At 26 hpf, the heart jogged to the left (C,F), to the right (E,H), or did not jog (D,G) in *charon* morphant embryos. Likewise, heart looping was disrupted in *charon* morphant embryos at 52 hpf (D-loop, I; no-loop, J; L-loop, K). (L) The *charon* morphant embryos showed no gross morphological abnormalities at 40 hpf. (A,B,L) Lateral views. (C-E, I-K) Ventral views. (F-H) Dorsal views.

embryos exhibited bilateral expression of all of these genes in the lateral plate during somitogenesis (Fig. 7B,E,H, Fig. 8B,E,H, Table 3). The effects of the *charon*-MO depended on the dose of the injected morpholino. We also observed bilateral expression of *atv/lefty1*, *cyc* and *pitx2* in the diencephalon in these embryos (Fig. 7B, Fig. 8B,E,H, Table 3); these are normally expressed only on the left side (Fig. 7A, Fig. 8A,D,G) (Concha et al., 2000; Essner et al., 2000; Liang et al., 2000; Rebagliati et al., 1998a; Sampath et al., 1998). The data indicate that Charon is required for the asymmetric expression of these genes in the LPM and the diencephalon.

Dorsal midline tissues are required to maintain L/R asymmetry ('midline barrier'). It is thought that *atv/lefty1* expression in the dorsal midline contributes to its barrier function (Meno et al., 1998). Defective midline development in zebrafish increases the incidence of bilateral expression of the left side-specific genes (Bisgrove et al., 2000; Danos and Yost, 1996). We examined the development of the midline tissues in the *charon* morphant embryos. Expression of *ntl* in the notochord and *sonic hedgehog* (*shh*) in the notochord (13 hpf) and floor plate (24 hpf) was not affected in the *charon* morphant embryos (Fig. 7L,M,O,S,U). There was also no discernible difference in *atv/lefty1* expression in the notochord and prechordal mesoderm at all somite stages examined (6-9 somite stage, Fig. 7Q; 12-13 and 17-20 somite stage, data not shown). We did not detect any morphological abnormality in the notochord and floor plate in these embryos (Fig. 7S,U). The data suggest that Charon is dispensable for the formation of the midline tissue and *atv/lefty1* expression in the midline. Because *charon* is expressed only in the regions adjacent to Kupffer's vesicle but not in the LPM or diencephalon, Charon probably functions in the early process of the L/R patterning, which takes place in or near Kupffer's vesicle.

Inhibition of Southpaw by Charon is required for the L/R patterning

Left-side expression of *spaw, pitx2, atv/lefty1* and *lefty2* is lost in embryos with reduced Spaw activity (Long et al., 2003). The same effects are seen in mouse mutant embryos that lack *nodal* expression in the node (Brennan et al., 2002; Saijoh et al., 2003), suggesting a role for Spaw and Nodal in the initial left-side determination. Because *charon* was co-expressed with *spaw* in the tail region and Charon inhibited Spaw's function in the misexpression study, we thought it probable that the antagonistic interaction between Charon and Spaw in the tail region plays a role in L/R patterning. To address this, we conducted an epistatic analysis using the MOs for *spaw* and *charon*. We examined the expression of *pitx2*, *atv/lefty1*, *lefty2* and *cyc* in embryos injected with both *spaw*-MO and *charon*-MO, or *charon*-MO alone. Injection of 0.8 ng of *charon*-MO occasionally increased the frequency of embryos expressing *pitx2*, *cyc*, *atv/lefty1* or *lefty2* on the right side, but most often led to bilateral expression of these genes in the LPM and diencephalon (for *pitx2*, *cyc* and *atv/lefty1*) (Fig. 8B,E,H, Table 3). Coinjection of 8 ng of *spaw*-MO with the *charon*-MO reduced or abolished the expression of these genes on both the left and right sides (Fig. 8C,F,I, Table 3). Because the same effect is observed in the *spaw* morphant embryos (Long et al., 2003), we conclude that *spaw* is epistatic to *charon* in the expression of the left-specific genes. These data provide additional evidence that Spaw functions as a left-side

Fig. 7. Charon is required for the early processes of L/R patterning. (A-I) Embryos were injected with *charon*-MO and examined for *atv/lefty1* (20 hpf, A-C), *spaw* (18 hpf, E-F), and *pitx2* (20 hpf, G-I) expression. In addition to the normal (left-sided) expression of the gene (A,D,G), bilateral (B,E,H) or reversed (C,F,I) expression of the left-side-specific markers was also observed. The numbers of embryos showing each phenotype are given in Table 3. Embryos that showed strong right-side stain and weaker left-side stain were recorded as bilateral (dorsal views). Arrowheads indicate the presence of the expression. (J-T) Midline barriers are not affected in *charon* morphant embryos. *no tail* (*ntl*) expression in notochord of wild-type (J,K) and *charon* morphant embryos (L,M) at 13 hpf. *sonic hedgehog* (*shh*) expression in notochord at 13 hpf (N,O) and in floor plate at 24 hpf (R,S) in wild-type (N,R) and *charon* morphant embryos (O,S). *antivin/lefty1* expression in wild-type (P) and *charon* morphant embryos (Q) at the 6-9-somite stage. Saggital sections of *ntl* expression at 24 hpf in wild-type (T) and *charon* morphant embryos (U). (J,L,R,S) Lateral views. (K,M,N,O) Dorsal views. (P,Q) Dorso-lateral views.
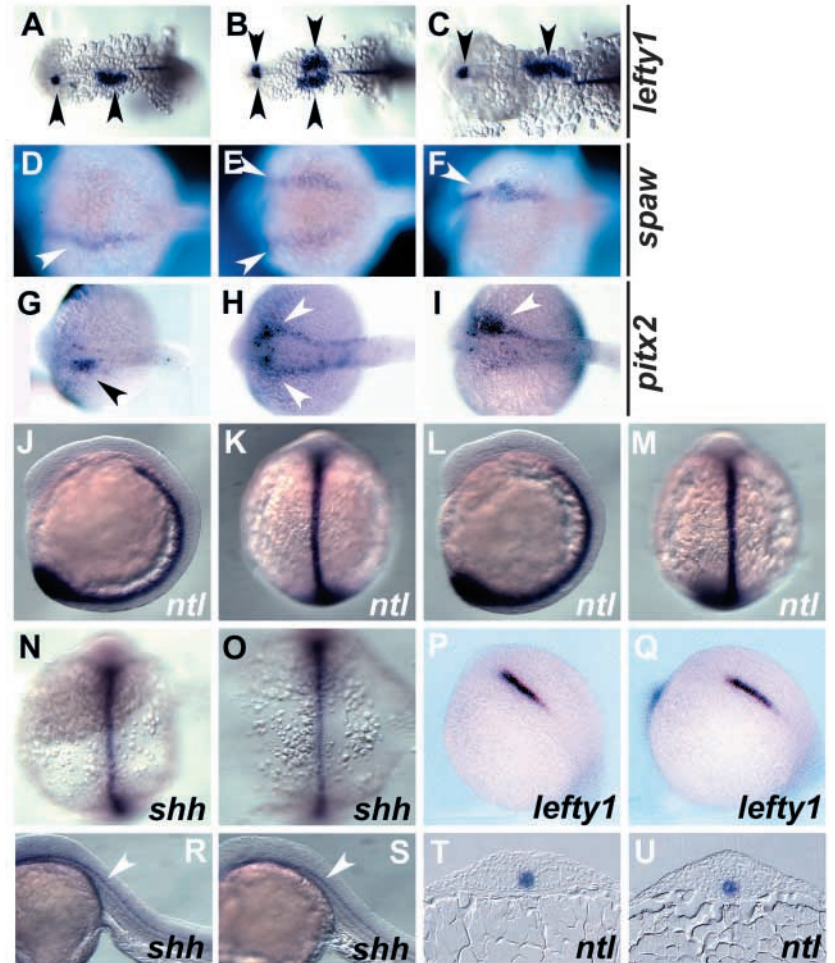
determinant and, more importantly, indicate a functional interaction between Charon and Spaw in the L/R patterning.

Discussion

Charon is a novel Nodal antagonist of the Cerberus/Caronte/Dan family

Many Cerberus/Dan family proteins, including Cerberus and Caronte, inhibit BMPs (reviewed by Balemans and Van Hul, 2002); only a subset of this family, including Cerberus and Coco, can inhibit all BMP, Nodal and Wnt signaling (Bell et al., 2003; Piccolo et al., 1999). In this study, we found that Charon inhibits Nodal signaling (Figs 4, 5). The misexpression of *charon* did not elicit dorsalization of the embryos (Fig. 4). Because BMP inhibition is sufficient to dorsalize the zebrafish embryos (Myers et al., 2002), our results suggest that Charon is not a strong BMP inhibitor. Caronte has been shown to function as a BMP inhibitor and transmit a left-side signal from the node to LPM (Rodriguez Esteban et al., 1999; Yokouchi et al., 1999). The net effect of Caronte is induction of *nodal* expression in the left LPM. Misexpression of *caronte* on the right side is

sufficient to induce ectopic *nodal* expression within the right LPM. We identified a novel role of Cerberus/Dan family proteins in L/R patterning that is very different from the role of Caronte. Our data show that Charon acts formally as a

Fig. 8. Southpaw is epistatic to Charon. Control (uninjected) embryos (A,D,G), and embryos injected with *charon*-MO (0.8 ng, B,E,H), or co-injected with *charon*-MO (0.8 ng) and *southpaw*-MO (8 ng) (*spaw*-MO+*charon*-MO, C,F,I), were examined for *pitx2* (22-24-somite stage, A-C), *cyclops* (*cyc*) (18-21-somite stage, D-F), and *antivin/lefty1* (18-21-somite stage, G-I) expression. (A-C) 'Face-on' views, optical sections. Similar effects were seen on *pitx2* expression in the lateral plate. Arrowheads indicate *pitx2* expression in dorsal diencephalons. (D-F) Dorsal views, with anterior to the top. Arrowheads indicate *cyc* expression in dorsal diencephalon and lateral plate mesoderm. (G-I) Dorsal views, with anterior to the left. Arrowheads indicate *antivin/lefty1* expression in dorsal diencephalon and lateral plate mesoderm. Typical data are shown in this Figure and the numbers showing laterality defects are given in Table 3.
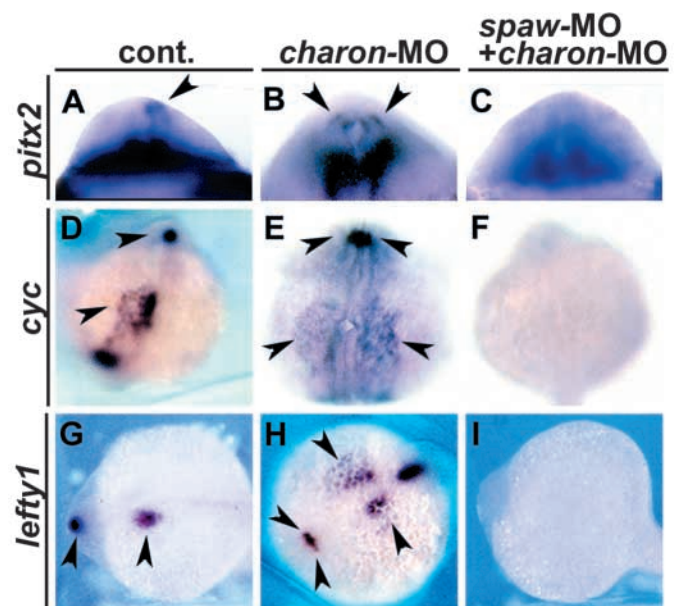
Table 3. Charon is required for early processes of the L/R patterning

Experiment	Morpholino	Dose (ng)	Marker	Stage (hpf)	n	Lateral plate (%)				Forebrain (%)			
						L	R	Bi	Ab	L	R	Bil	Ab
1	4-Mis	0.4	*lefty1*	18-21	88	98	1	1	0				
	charon-MO	0.4	*lefty1*	18-21	94	45	17	23	0				
	4-Mis	0.8	*lefty1*	18-21	67	99	0	1	0				
	charon-MO	0.8	*lefty1*	18-21	121	46	23	31	0				
2	4-Mis	0.4	*pitx2*	22-24	68	97	0	3	0				
	charon-MO	0.4	*pitx2*	22-24	83	47	39	14	0				
	4-Mis	0.8	*pitx2*	22-24	95	97	2	1	0				
	charon-MO	0.8	*pitx2*	22-24	138	28	10	62	0				
3	4-Mis	0.4	*spaw*	15-17	30	90	3	7	0				
	charon-MO	0.4	*spaw*	15-17	59	49	10	41	0				
	4-Mis	0.8	*spaw*	15-17	69	86	3	12	0				
	charon-MO	0.8	*spaw*	15-17	38	18	11	71	0				
4	None		*lefty1*	18-21	53	64	0	0	36	91	0	0	9
	charon-MO	0.8	*lefty1*	18-21	25	12	4	40	44	20	8	20	52
	spaw-MO+*charon*-MO	8+0.8	*lefty1*	18-21	25	0	0	0	100	4	0	0	96
5	None		*lefty2*	23-24	77	100	0	0	0				
	charon-MO	0.8	*lefty2*	18-24	22	13	23	64	0				
	spaw-MO+*charon*-MO	8+0.8	*lefty2*	20-23	25	0	0	0	100				
6	None		*cyclops*	18-20	50	64	0	0	36	78	0	8	14
	charon-MO	0.8	*cyclops*	18-20	49	12	4	74	10	14	6	62	18
	spaw-MO+*charon*-MO	8+0.8	*cyclops*	18-20	48	4	0	0	96	0	0	0	100
7	None		*pitx2*	22-24	55	93	0	0	7	85	0	11	4
	charon-MO	0.8	*pitx2*	22-24	50	20	0	80	0	28	2	62	8
	spaw-MO+*charon*-MO	8+0.8	*pitx2*	22-24	41	2	2	6	90	7	0	0	93

charon-MO, control MO (4-Mis), or a combination of *spaw*-MO and *charon*-MO were injected and the embryos were stained for with *atv/lefty1*, *lefty2*, *cyc*, *spaw* and *pitx2*. Numbers (%) of the embryos showing left (L), right (R), bilateral (Bi) and absent (Ab) expression of these markers are shown.

negative regulator of Nodal expression within the right LPM, because loss of Charon function results in *southpaw* (*nodal*) expression within both the right and left LPM (Fig. 7, Table 3). The Charon-deficient embryos had a normal notochord and floor plate and maintained the normal *atv/lefty1*-dependent midline barrier. This suggests that Charon acts within or near Kupffer's vesicle to help restrict or counteract left-biased signals generated in or near Kupffer's vesicle. This would be opposite to the proposed effect of Caronte, which is to facilitate or mediate the transmission of a left-side signal from the node to LPM. The different modes of action of Charon and Caronte are consistent with the low absolute level of sequence similarity between these two proteins (Fig. 1). In addition, *charon* displayed a very different expression profile from *cerberus* and *caronte*, which are expressed in the deep endomesoderm and head mesenchyme in *Xenopus* embryos and in the left paraxial mesoderm and LPM in the segmentation stage in chick embryos, respectively, supporting the idea that Charon is a novel member of the Cerberus/Dan family proteins.

One of the Cerberus/Dan family proteins, mouse *dante*, is expressed in the definitive node from the bud stage (Pearce et al., 1999). *dante* expression in the mouse node is very similar to *charon* expression in the Kupffer's vesicle region of the zebrafish, suggesting that Dante is an orthologue of Charon. However, only a partial sequence of *dante* has been reported and its biochemical function is not yet known, although it has been suggested that Dante functions as a Nodal inhibitor (Brennan et al., 2002). Thus, the relationship between Charon and Dante remains to be elucidated. Future comparison between the zebrafish *charon* morphant embryos and *dante*-deficient mouse embryos, and biochemical

analysis of Dante activity against Nodal will clarify this point.

In the mouse, *dante* and *nodal* are initially expressed symmetrically in the node region, and the *dante* expression becomes stronger on the right side of the node by early somitogenesis, in contrast to the stronger expression of *nodal* on the left side (Collignon et al., 1996; Pearce et al., 1999). We observed that the majority of embryos showed symmetric expression of *charon* (Fig. 2), implicating that the regulation of *charon* is different from that of *dante* in mouse. However, it could not be excluded that *charon* shows right-biased expression transiently.

Atv/Lefty1 and Lefty2, members of TGF-β family, function as feedback inhibitors for Nodal signaling (Cheng et al., 2000; Meno et al., 1999; Sakuma et al., 2002). *atv/lefty1* is expressed in the Kupffer's vesicle region during early somitogenesis, and its expression is abrogated in *oep* mutant embryos (Bisgrove et al., 1999), suggesting that the *atv/lefty1* expression in the Kupffer's vesicle region depends on Nodal signaling. The *charon* expression in the Kupffer's vesicle region was dependent on the Nodal signaling. The expression of *charon* was abolished or strongly reduced in the *sqt* and *atv/lefty1*-injected embryos (Fig. 3), which display defective development of Kupffer's vesicle (Dougan et al., 2003). The *charon* expression was not affected in the *cyc* embryos, and was reduced in the *oep* embryos, with the severity of the decrease correlating with the reduction in the size of Kupffer's vesicle. These data suggest that the *charon* expression depends on the formation of Kupffer's vesicle and that Nodal signaling indirectly regulates the *charon* expression. Consistent with this, the *charon* expression was abrogated or strongly reduced in the

boz and *ntl* mutant embryos (Fig. 3), which have defects in the formation of Kupffer's vesicle (Fekany et al., 1999; Melby et al., 1996). However, because the aforementioned mutants also affect other aspects of mesendoderm development, we cannot rule out the possibility that the *charon* expression is regulated by a signal distinct from those that induce morphological development of Kupffer's vesicle. Our data indicate that Charon functions to restrict laterality near Kupffer's vesicle, probably in cooperation with Atv/Lefty1.

Antagonistic interactions between Charon and Southpaw

Three lines of evidence argue that Southpaw is a physiological target for Charon. First, Charon interacted with Spaw biochemically and the dorsalizing activity of Spaw was inhibited by the overexpression of Charon (Fig. 5). Second, the expression domains of *charon* and *spaw* were in close proximity to each other in the tail region (Fig. 5), and both genes encode secreted proteins that will probably be secreted into overlapping regions. Third, the loss-of-function experiments showed that Spaw is epistatic to Charon in the expression of the left side-specific genes (Fig. 8, Table 3) in both the LPM and diencephalon. All of these data suggest that the inhibition of Spaw by Charon is involved in the generation of embryonic L/R asymmetry. The inhibition of Spaw's function leads to a reduction or loss of left side-specific gene expression (Long et al., 2003), suggesting that Spaw functions as a left-side determinant, as proposed for Nodal in mouse (Hamada et al., 2002). However, *spaw* is expressed not only in the Kupffer's vesicle region but also in the left LPM. The functional relevance of Spaw in the Kupffer's vesicle region has not been tested yet, as the *spaw*-MOs would block Spaw activity in all the *spaw* expression domains. In this study, Charon, which is expressed in Kupffer's vesicle, interacted functionally with Spaw, suggesting that Spaw may function in the Kupffer's vesicle region to initiate left-side determination. However, there is one significant argument against this idea: in *ntl* mutants, *spaw* expression domains in Kupffer's vesicle are lost, but *spaw* is expressed bilaterally in the LPM (Long et al., 2003), suggesting that Spaw in the Kupffer's vesicle region is not required for the expression of Spaw in the LPM. The situation is different from *nodal* in the mouse; elimination of *nodal* in the node region disrupts *nodal* expression in the left LPM in the mouse (Brennan et al., 2002; Saijoh et al., 2003).

There are several possible explanations for this discrepancy. First, a low level of Spaw could be transiently expressed in the Kupffer's vesicle region in the *ntl* mutant embryos and induce *spaw* expression in the LPM in the absence of the midline barriers and the Nodal inhibitor Charon. Second, if Nodal-class proteins turn over slowly, then pre-existing Nodal proteins, such as Cyc and Sqt, might compensate for the loss of Spaw in the Kupffer's vesicle region in the *ntl* mutant embryos. Consistent with this possibility, in *ntl* mutants, *cyc* expression is lost in the tailbud but is concomitantly upregulated or shifted into posterior-lateral territories at the bud stage (Rebagliati et al., 1998a). Charon could inhibit the dorsalizing activity of Cyc (Fig. 5). We could not exclude the possibility that there is a non-Nodal factor, possibly another TGF-β, which is expressed in the Kupffer's vesicle region and activates Nodal signaling in the LPM in the *ntl* mutant. In mouse, GDF1 expression in the node is required for the expression of *nodal, lefty2* and *pitx2* in the left LPM (Rankin et al., 2000). It is also possible that, in the absence of a midline barrier and Charon, *spaw* could be expressed in the LPM by a constitutive or default mechanism.

Role for Charon in L/R asymmetry

Loss of the Charon function by the morpholino-mediated inhibition led to bilateral expression of the left side-specific genes and randomization of heart jogging and looping (Figs 6, 7, Table 2). In this sense, the phenotypes of the *charon* morphant embryos are similar to those observed in zebrafish mutants *boz* (*momo*), *ntl* and *flh*, which have defects in the formation of midline structures (Bisgrove et al., 2000; Long et al., 2003), and in mutant mice deficient in *lefty1*, which is expressed in the left floor plate (Meno et al., 1998), raising the question as to whether Charon is involved in the formation of 'the midline barrier'. However, the development of midline tissues, such as notochord and floor plate, and the expression of *ntl, shh* and *atv/lefty1* were not affected in the *charon* morphant embryos (Fig. 7), suggesting that Charon is dispensable for the formation of the midline barrier. We cannot completely rule out the possibility that Charon is involved in expression or function of an unidentified component(s) of the midline barrier. Because *charon* is expressed only in the Kupffer's vesicle region, we favor the hypothesis that Charon functions near Kupffer's vesicle rather than regulating midline barrier functions of the notochord or floor plate.

lr dynein-related is expressed in the dorsal forerunner cells, and cells within Kupffer's vesicle have a cilium, in zebrafish (Essner et al., 2002), suggesting that Kupffer's vesicle is equivalent to the node cavity in mouse. Likewise, the fact that asymmetric expression of the *nodal*-related gene *spaw* begins near Kupffer's vesicle, and that this pattern is disrupted by mutations that affect forerunner cells, also supports this equivalence (Long et al., 2003). It has not yet been reported whether the cilia in the Kupffer's vesicle rotate and generate the leftward flow (nodal flow) in zebrafish. It has also not yet been shown whether the L/R signal is initiated in Kupffer's vesicle in zebrafish. Here, we have demonstrated that *charon* is expressed in or next to Kupffer's vesicle and that Charon functions in the L/R patterning without affecting the development of the midline tissue and *atv/lefty1*-dependent midline barrier, suggesting that L/R patterning is initiated in the Kupffer's vesicle region. Given that loss of molecular components of the mouse node and zebrafish Kupffer's vesicle can result in similar L/R defects, our data provide support for the proposal that these structures are functionally equivalent and that they have an evolutionarily conserved role in L/R patterning (Essner et al., 2002). It is tempting to speculate that Nodal-related molecule(s) such as Spaw (or possibly Cyc) function in the Kupffer's vesicle region in zebrafish in the same way as had been proposed for Nodal protein in the perinodal region in mice. In this scenario, the Nodal signaling is biased to the left side of the Kupffer's vesicle region in zebrafish. Charon might be involved in creating an 'all or nothing' condition of Nodal signaling on each side of the Kupffer's vesicle region by reducing the Nodal signaling baseline.

In this study, we isolated Charon, a novel player in L/R patterning, and found antagonistic interactions between Charon and Nodal (Southpaw) to be involved in L/R patterning. This finding sheds new light on the role of

References

Balemans, W. and Van Hul, W. (2002). Extracellular regulation of BMP signaling in vertebrates: a cocktail of modulators. *Dev. Biol.* **250**, 231-250.

Bell, E., Munoz-Sanjuan, I., Altmann, C. R., Vonica, A. and Brivanlou, A. H. (2003). Cell fate specification and competence by Coco, a maternal BMP, TGFβ and Wnt inhibitor. *Development* **130**, 1381-1389.

Bisgrove, B. W., Essner, J. J. and Yost, H. J. (1999). Regulation of midline development by antagonism of *lefty* and *nodal* signaling. *Development* **126**, 3253-3262.

Bisgrove, B. W., Essner, J. J. and Yost, H. J. (2000). Multiple pathways in the midline regulate concordant brain, heart and gut left-right asymmetry. *Development* **127**, 3567-3579.

Brennan, J., Norris, D. P. and Robertson, E. J. (2002). Nodal activity in the node governs left-right asymmetry. *Genes Dev.* **16**, 2339-2344.

Burdine, R. D. and Schier, A. F. (2000). Conserved and divergent mechanisms in left-right axis formation. *Genes Dev.* **14**, 763-776.

Chen, J. N. and Fishman, M. C. (1996). Zebrafish *tinman* homolog demarcates the heart field and initiates myocardial differentiation. *Development* **122**, 3809-3816.

Chen, J. N., van Eeden, F. J., Warren, K. S., Chin, A., Nusslein-Volhard, C., Haffter, P. and Fishman, M. C. (1997). Left-right pattern of cardiac BMP4 may drive asymmetry of the heart in zebrafish. *Development* **124**, 4373-4382.

Cheng, A. M., Thisse, B., Thisse, C. and Wright, C. V. (2000). The lefty-related factor Xatv acts as a feedback inhibitor of Nodal signaling in mesoderm induction and L-R axis development in *Xenopus*. *Development* **127**, 1049-1061.

Chin, A. J., Tsang, M. and Weinberg, E. S. (2000). Heart and gut chiralities are controlled independently from initial heart position in the developing zebrafish. *Dev. Biol.* **227**, 403-421.

Collignon, J., Varlet, I. and Robertson, E. J. (1996). Relationship between asymmetric *nodal* expression and the direction of embryonic turning. *Nature* **381**, 155-158.

Concha, M. L., Burdine, R. D., Russell, C., Schier, A. F. and Wilson, S. W. (2000). A Nodal signaling pathway regulates the laterality of neuroanatomical asymmetries in the zebrafish forebrain. *Neuron* **28**, 399-409.

Cooper, M. S. and D'Amico, L. A. (1996). A cluster of noninvoluting endocytic cells at the margin of the zebrafish blastoderm marks the site of embryonic shield formation. *Dev. Biol.* **180**, 184-198.

Danos, M. C. and Yost, H. J. (1996). Role of notochord in specification of cardiac left-right orientation in zebrafish and *Xenopus*. *Dev. Biol.* **177**, 96-103.

Dougan, S. T., Warga, R. M., Kane, D. A., Schier, A. F. and Talbot, W. S. (2003). The role of the zebrafish *nodal*-related genes *squint* and *cyclops* in patterning of mesendoderm. *Development* **130**, 1837-1851.

Essner, J. J., Branford, W. W., Zhang, J. and Yost, H. J. (2000). Mesendoderm and left-right brain, heart and gut development are differentially regulated by *pitx2* isoforms. *Development* **127**, 1081-1093.

Essner, J. J., Vogan, K. J., Wagner, M. K., Tabin, C. J., Yost, H. J. and Brueckner, M. (2002). Conserved function for embryonic nodal cilia. *Nature* **418**, 37-38.

Fekany, K., Yamanaka, Y., Leung, T., Sirotkin, H. I., Topczewski, J.,

Gates, M. A., Hibi, M., Renucci, A., Stemple, D., Radbill, A. et al. (1999). The zebrafish *bozozok* locus encodes Dharma, a homeodomain protein essential for induction of gastrula organizer and dorsoanterior embryonic structures. *Development* **126**, 1427-1438.

Feldman, B., Gates, M. A., Egan, E. S., Dougan, S. T., Rennebeck, G., Sirotkin, H. I., Schier, A. F. and Talbot, W. S. (1998). Zebrafish organizer development and germ-layer formation require nodal-related signals. *Nature* **395**, 181-185.

Fujiwara, T., Dehart, D. B., Sulik, K. K. and Hogan, B. L. (2002). Distinct requirements for extra-embryonic and embryonic bone morphogenetic protein 4 in the formation of the node and primitive streak and coordination of left-right asymmetry in the mouse. *Development* **129**, 4685-4696.

Furthauer, M., Thisse, B. and Thisse, C. (1999). Three different *noggin* genes antagonize the activity of bone morphogenetic proteins in the zebrafish embryo. *Dev. Biol.* **214**, 181-196.

Gamse, J. T., Thisse, C., Thisse, B. and Halpern, M. E. (2003). The parapineal mediates left-right asymmetry in the zebrafish diencephalon. *Development* **130**, 1059-1068.

Gritsman, K., Zhang, J., Cheng, S., Heckscher, E., Talbot, W. S. and Schier, A. F. (1999). The EGF-CFC protein one-eyed pinhead is essential for Nodal signaling. *Cell* **97**, 121-132.

Hamada, H., Meno, C., Saijoh, Y., Adachi, H., Yashiro, K., Sakuma, R. and Shiratori, H. (2001). Role of asymmetric signals in left-right patterning in the mouse. *Am. J. Med. Genet.* **101**, 324-327.

Hamada, H., Meno, C., Watanabe, D. and Saijoh, Y. (2002). Establishment of vertebrate left-right asymmetry. *Nat. Rev. Genet.* **3**, 103-113.

Hashimoto, H., Itoh, M., Yamanaka, Y., Yamashita, S., Shimizu, T., Solnica-Krezel, L., Hibi, M. and Hirano, T. (2000). Zebrafish Dkk1 functions in forebrain specification and axial mesendoderm formation. *Dev. Biol.* **217**, 138-152.

Hashimoto, H., Mizuta, A., Okada, N., Suzuki, T., Tagawa, M., Tabata, K., Yokoyama, Y., Sakaguchi, M., Tanaka, M. and Toyohara, H. (2002). Isolation and characterization of a Japanese flounder clonal line, *reversed*, which exhibits reversal of metamorphic left-right asymmetry. *Mech. Dev.* **111**, 17-24.

Kramer, K. L., Barnette, J. E. and Yost, H. J. (2002). PKCgamma regulates syndecan-2 inside-out signaling during *Xenopus* left-right development. *Cell* **111**, 981-990.

Levin, M. and Mercola, M. (1999). Gap junction-mediated transfer of left-right patterning signals in the early chick blastoderm is upstream of Shh asymmetry in the node. *Development* **126**, 4703-4714.

Levin, M., Thorlin, T., Robinson, K. R., Nogi, T. and Mercola, M. (2002). Asymmetries in H+/K+-ATPase and cell membrane potentials comprise a very early step in left-right patterning. *Cell* **111**, 77-89.

Liang, J. O., Etheridge, A., Hantsoo, L., Rubinstein, A. L., Nowak, S. J., Izpisua Belmonte, J. C. and Halpern, M. E. (2000). Asymmetric Nodal signaling in the zebrafish diencephalon positions the pineal organ. *Development* **127**, 5101-5112.

Lohr, J. L., Danos, M. C. and Yost, H. J. (1997). Left-right asymmetry of a *nodal*-related gene is regulated by dorsoanterior midline structures during *Xenopus* development. *Development* **124**, 1465-1472.

Long, S., Ahmad, N. and Rebagliati, M. (2002). Zebrafish hearts and minds: nodal signaling in cardiac and neural left-right asymmetry. *Cold Spring Harbor Symp. Quant. Biol.* **67**, 27-36.

Long, S., Ahmad, N. and Rebagliati, M. (2003). The zebrafish *nodal*-related gene *southpaw* is required for visceral and diencephalic left-right asymmetry. *Development* **130**, 2303-2316.

Long, S. and Rebagliati, M. (2002). Sensitive two-color whole-mount in situ hybridizations using digoxygenin- and dinitrophenol-labeled RNA probes. *BioTechniques* **32**, 494-500.

McGrath, J., Somlo, S., Makova, S., Tian, X. and Brueckner, M. (2003). Two populations of node monocilia initiate left-right asymmetry in the mouse. *Cell* **114**, 61-73.

Melby, A. E., Warga, R. M. and Kimmel, C. B. (1996). Specification of cell fates at the dorsal margin of the zebrafish gastrula. *Development* **122**, 2225-2237.

Meno, C., Gritsman, K., Ohishi, S., Ohfuji, Y., Heckscher, E., Mochida, K., Shimono, A., Kondoh, H., Talbot, W. S., Robertson, E. J. et al. (1999). Mouse Lefty2 and zebrafish Antivin are feedback inhibitors of nodal signaling during vertebrate gastrulation. *Mol. Cell* **4**, 287-298.

Meno, C., Shimono, A., Saijoh, Y., Yashiro, K., Mochida, K., Ohishi, S., Noji, S., Kondoh, H. and Hamada, H. (1998). *lefty-1* is required for left-right determination as a regulator of *lefty-2* and *nodal*. *Cell* **94**, 287-297.

Miller-Bertoglio, V. E., Fisher, S., Sanchez, A., Mullins, M. C. and Halpern, M. E. (1997). Differential regulation of *chordin* expression domains in mutant zebrafish. *Dev. Biol.* **192**, 537-550.

Myers, D. C., Sepich, D. S. and Solnica-Krezel, L. (2002). Bmp activity gradient regulates convergent extension during zebrafish gastrulation. *Dev. Biol.* **243**, 81-98.

Nasevicius, A. and Ekker, S. C. (2000). Effective targeted gene 'knockdown' in zebrafish. *Nat. Genet.* **26**, 216-220.

Nonaka, S., Tanaka, Y., Okada, Y., Takeda, S., Harada, A., Kanai, Y., Kido, M. and Hirokawa, N. (1998). Randomization of left-right asymmetry due to loss of nodal cilia generating leftward flow of extraembryonic fluid in mice lacking KIF3B motor protein. *Cell* **95**, 829-837.

Norris, D. P., Brennan, J., Bikoff, E. K. and Robertson, E. J. (2002). The Foxh1-dependent autoregulatory enhancer controls the level of Nodal signals in the mouse embryo. *Development* **129**, 3455-3468.

Okada, Y., Nonaka, S., Tanaka, Y., Saijoh, Y., Hamada, H. and Hirokawa, N. (1999). Abnormal nodal flow precedes situs inversus in *iv* and *inv* mice. *Mol. Cell* **4**, 459-468.

Osada, S. I., Saijoh, Y., Frisch, A., Yeo, C. Y., Adachi, H., Watanabe, M., Whitman, M., Hamada, H. and Wright, C. V. (2000). Activin/Nodal responsiveness and asymmetric expression of a *Xenopus nodal*-related gene converge on a FAST-regulated module in intron 1. *Development* **127**, 2503-2514.

Pearce, J. J., Penny, G. and Rossant, J. (1999). A mouse cerberus/Dan-related gene family. *Dev. Biol.* **209**, 98-110.

Piccolo, S., Agius, E., Leyns, L., Bhattacharyya, S., Grunz, H., Bouwmeester, T. and De Robertis, E. M. (1999). The head inducer Cerberus is a multifunctional antagonist of Nodal, BMP and Wnt signals. *Nature* **397**, 707-710.

Piedra, M. E. and Ros, M. A. (2002). BMP signaling positively regulates Nodal expression during left right specification in the chick embryo. *Development* **129**, 3431-3440.

Pogoda, H. M., Solnica-Krezel, L., Driever, W. and Meyer, D. (2000). The zebrafish forkhead transcription factor FoxH1/Fast1 is a modulator of Nodal signaling required for organizer formation. *Curr. Biol.* **10**, 1041-1049.

Rankin, C. T., Bunton, T., Lawler, A. M. and Lee, S. J. (2000). Regulation of left-right patterning in mice by growth/differentiation factor-1. *Nat. Genet.* **24**, 262-265.

Rebagliati, M. R., Toyama, R., Fricke, C., Haffter, P. and Dawid, I. B. (1998a). Zebrafish nodal-related genes are implicated in axial patterning and establishing left-right asymmetry. *Dev. Biol.* **199**, 261-272.

Rebagliati, M. R., Toyama, R., Haffter, P. and Dawid, I. B. (1998b). *cyclops* encodes a nodal-related factor involved in midline signaling. *Proc. Natl. Acad. Sci. USA* **95**, 9932-9937.

Rodriguez Esteban, C., Capdevila, J., Economides, A. N., Pascual, J., Ortiz, A. and Izpisua Belmonte, J. C. (1999). The novel Cer-like protein Caronte mediates the establishment of embryonic left-right asymmetry. *Nature* **401**, 243-251.

Saijoh, Y., Adachi, H., Sakuma, R., Yeo, C. Y., Yashiro, K., Watanabe, M., Hashiguchi, H., Mochida, K., Ohishi, S., Kawabata, M. et al. (2000). Left-right asymmetric expression of *lefty2* and *nodal* is induced by a signaling pathway that includes the transcription factor FAST2. *Mol. Cell* **5**, 35-47.

Saijoh, Y., Oki, S., Ohishi, S. and Hamada, H. (2003). Left-right patterning of the mouse lateral plate requires nodal produced in the node. *Dev. Biol.* **256**, 161-173.

Sakuma, R., Ohnishi Yi, Y., Meno, C., Fujii, H., Juan, H., Takeuchi, J., Ogura, T., Li, E., Miyazono, K. and Hamada, H. (2002). Inhibition of

Nodal signalling by Lefty mediated through interaction with common receptors and efficient diffusion. *Genes Cells* **7**, 401-412.

Sampath, K., Rubinstein, A. L., Cheng, A. M., Liang, J. O., Fekany, K., Solnica-Krezel, L., Korzh, V., Halpern, M. E. and Wright, C. V. (1998). Induction of the zebrafish ventral brain and floorplate requires cyclops/nodal signalling. *Nature* **395**, 185-189.

Schlange, T., Arnold, H. H. and Brand, T. (2002). BMP2 is a positive regulator of Nodal signaling during left-right axis formation in the chicken embryo. *Development* **129**, 3421-3429.

Schlange, T., Schnipkoweit, I., Andree, B., Ebert, A., Zile, M. H., Arnold, H. H. and Brand, T. (2001). Chick CFC controls Lefty1 expression in the embryonic midline and nodal expression in the lateral plate. *Dev. Biol.* **234**, 376-389.

Shinya, M., Eschbach, C., Clark, M., Lehrach, H. and Furutani-Seiki, M. (2000). Zebrafish Dkk1, induced by the pre-MBT Wnt signaling, is secreted from the prechordal plate and patterns the anterior neural plate. *Mech. Dev.* **98**, 3-17.

Shiratori, H., Sakuma, R., Watanabe, M., Hashiguchi, H., Mochida, K., Sakai, Y., Nishino, J., Saijoh, Y., Whitman, M. and Hamada, H. (2001). Two-step regulation of left-right asymmetric expression of *Pitx2*: initiation by Nodal signaling and maintenance by Nkx2. *Mol. Cell* **7**, 137-149.

Sirotkin, H. I., Gates, M. A., Kelly, P. D., Schier, A. F. and Talbot, W. S. (2000). Fast1 is required for the development of dorsal axial structures in zebrafish. *Curr. Biol.* **10**, 1051-1054.

Solnica-Krezel, L., Stemple, D. L., Mountcastle-Shah, E., Rangini, Z., Neuhauss, S. C., Malicki, J., Schier, A. F., Stainier, D. Y., Zwartkruis, F., Abdelilah, S. et al. (1996). Mutations affecting cell fates and cellular rearrangements during gastrulation in zebrafish. *Development* **123**, 67-80.

Supp, D. M., Witte, D. P., Potter, S. S. and Brueckner, M. (1997). Mutation of an axonemal dynein affects left-right asymmetry in *inversus viscerum* mice. *Nature* **389**, 963-966.

Suzuki, T., Kurokawa, T., Hashimoto, H. and Sugiyama, M. (2002). cDNA sequence and tissue expression of *Fugu rubripes* prion protein-like: a candidate for the teleost orthologue of tetrapod PrPs. *Biochem. Biophys. Res. Commun.* **294**, 912-917.

Tabin, C. J. and Vogan, K. J. (2003). A two-cilia model for vertebrate left-right axis specification. *Genes Dev.* **17**, 1-6.

Thisse, C. and Thisse, B. (1999). Antivin, a novel and divergent member of the TGFβ superfamily, negatively regulates mesoderm induction. *Development* **126**, 229-240.

Wright, C. V. (2001). Mechanisms of left-right asymmetry: what's right and what's left? *Dev. Cell* **1**, 179-186.

Wright, C. V. and Halpern, M. E. (2002). Specification of left-right asymmetry. *Results Probl. Cell Differ.* **40**, 96-116.

Yan, Y. T., Gritsman, K., Ding, J., Burdine, R. D., Corrales, J. D., Price, S. M., Talbot, W. S., Schier, A. F. and Shen, M. M. (1999). Conserved requirement for *EGF-CFC* genes in vertebrate left-right axis formation. *Genes Dev.* **13**, 2527-2537.

Yelon, D., Horne, S. A. and Stainier, D. Y. (1999). Restricted expression of cardiac myosin genes reveals regulated aspects of heart tube assembly in zebrafish. *Dev. Biol.* **214**, 23-37.

Yokouchi, Y., Vogan, K. J., Pearse, R. V., 2nd and Tabin, C. J. (1999). Antagonistic signaling by *Caronte*, a novel *Cerberus*-related gene, establishes left-right asymmetric gene expression. *Cell* **98**, 573-583.

Yoshioka, H., Meno, C., Koshiba, K., Sugihara, M., Itoh, H., Ishimaru, Y., Inoue, T., Ohuchi, H., Semina, E. V., Murray, J. C. et al. (1998). *Pitx2*, a bicoid-type homeobox gene, is involved in a lefty-signaling pathway in determination of left-right asymmetry. *Cell* **94**, 299-305.

Yost, H. J. (1998). Left-right development in *Xenopus* and zebrafish. *Semin. Cell Dev. Biol.* **9**, 61-66.